JOURNAL OF GUIDANCE, CONTROL, AND DYNAMICS
Vol. 21, No. 6, November–December 1998

Near-Optimal Entry Trajectories for Reusable Launch Vehicles

H.-C. Chou* and M. D. Ardema†
Santa Clara University, Santa Clara, California 95053
and
J. V. Bowles‡
NASA Ames Research Center, Moffet Field, California 94035

A near-optimal guidance law for the descent trajectory of a fully reusable single-stage-to-orbit rocket launch vehicle is derived. A methodology is developed to investigate using both bank angle and altitude as control variables and selecting parameters that maximize various performance functions. The method is based on the energy-state model of the aircraft equations of motion. The major task of this paper is to obtain optimal entry trajectories under a variety of performance goals: minimum time, minimum surface temperature, minimum heat load, and maximum heading change. Four classes of trajectories were investigated: no banking, optimal left turn banking, optimal right turn banking, and optimal bank chattering. The cost function is in general a weighted sum of all performance goals. In particular, the tradeoff between minimizing heat load into the vehicle and maximizing cross-range distance is investigated. The results show that the optimization methodology can be used to derive a wide variety of near-optimal trajectories.

Nomenclature

D = drag, lb
E = total mechanical energy per unit weight, ft
e = emissivity
g = gravitational acceleration at altitude, ft/s^2
g_s = gravitational acceleration on the Earth's surface, ft/s^2
h = altitude, ft
K = weighting parameter, lb/ft^3
L = lift, lb
M = Mach number
m = aircraft mass, slugs
Q = heat load, Btu/h
$\dot{Q}$ = convective heat transfer rate, Btu/h/ft^2
q = dynamic pressure, lb/ft^2
R = radius of the Earth, ft
T_{amb} = ambient temperature, °R
T_{surf} = surface temperature, °R
t = time, s
V = speed, ft/s
W = aircraft Earth surface weight (mass), lb
X = longitudinal range over Earth's surface, ft
Y = latitudinal range over Earth's surface, ft
α = angle of attack, rad
γ = flight-path angle, rad
σ = Boltzman constant, Btu/ft^2-s-°R^4
ϕ = bank angle, rad
χ = heading angle, rad
ω = Earth's rotational angular velocity, rad/s

I. Introduction

A NATIONAL program is under way to identify and to develop the best launch vehicle and transportation architectures to make major reductions in the cost of space transportation while at the same time increasing safety for flight crews. Attention has focused on a single-stage-to-orbit (SSTO), rocket-powered, fully reusable launch vehicle.[1,2] Missions being studied include satellite servicing and deployment and space station logistics delivery/return with flight crew rotations. This paper studies an optimal entry guidance law for such a vehicle.

One of the key objectives of entry trajectory optimization is to fly the vehicle to the desired ground destination while limiting heat load and deceleration. The interest in turning trajectories arises from abort requirements, particularly the need to return to the launch site after one orbit. The heating environment to which the vehicle is exposed is one of the challenging problems for hypersonic flight control. Because high angles of attack required for turning increase the vehicle's surface temperatures, abort trajectories are the cases that typically size the thermal protection system. What is desirable is a flight path that results in sufficient cross range while minimizing heating subject to temperature limits on the vehicle surface. A major goal of this paper is to determine trajectories that minimize heat load or maximize turning capability or a weighted combination of the two.

There has been significant recent research in trajectory optimization and guidance of advanced launch vehicles (for example, Refs. 3–12). In Ref. 3, a linear feedback control law is used for trajectory control, with the gain scheduled with energy state. Reference 4 proposes using an autonomous guidance scheme using a nonlinear programming algorithm with a self-targeting capability. Similar to the present paper, Refs. 5, 6, and 10–12 employ energy as a state variable for determining near-optimal ascent and descent trajectories. References 7 and 9 have considered the need to limit the heat load on the vehicle.

Application of optimal control theory in the form of the maximum principle to aircraft trajectory optimization problems results in a two-point-boundary-value problem. The order of this problem is double the number of state variables, and the equations are always half unstable. Many schemes have been developed to numerically solve this difficult class of problem, but all are unsuitable in a vehicle synthesis study. Although there are well-developed numerical methods for trajectory optimization of point-mass vehicle models, these methods are too expensive computationally and not robust enough to be used at the conceptual design stage, in which many hundreds of vehicle designs must be evaluated and compared on a consistent basis.

What is needed in a vehicle synthesis study is a method that optimizes the trajectory in one pass, i.e., one that is an integral part of the trajectory integration. The method must also be robust,

Received Oct. 20, 1997; revision received May 15, 1998; accepted for publication May 18, 1998.

*Graduate Research Assistant, Department of Mechanical Engineering; also, currently Project Manager, Applied Materials, Hsih-Chu, Taiwan 300, Republic of China. Student Member AIAA.
†Professor and Chairman, Department of Mechanical Engineering. Associate Fellow AIAA.
‡Aerospace Engineer, System Analysis Branch. Member AIAA.

and it should be easy to use and to interpret physically. The key to achieving this is to use judicious approximations that reduce the system dynamics to a single state equation, thereby replacing the functional optimization problem by a function one.

In this paper, the energy state approximation (ESA) is used to obtain optimal trajectories. This well-known technique substitutes the total mechanical energy for the speed as a state variable and then neglects the altitude and flight-path dynamics relative to the energy dynamics. Formally, this may be viewed as the use of the singular perturbation theory to timescale decouple the equations of motion. When flight-path optimization is done with the ESA model, simple rules for the optimal trajectory are obtained. This dynamic model has been used successfully many times to obtain effective guidance laws for a wide variety of aircraft and missions.

In a series of papers Ardema et al.[8,10–12] have used energy-state methods to develop algorithms for ascent trajectory optimization and optimal operation of propulsion systems of advanced launch vehicles. The present paper extends these methods to enable computation of near-optimal entry trajectories for minimum time, minimum heat load, minimum surface temperature, maximum heading angle rate, or a combination of these.

In the numerical results, vehicle performance is computed using the NASA Ames hypersonic aircraft vehicle optimization code (HAVOC). HAVOC integrates geometry, aerodynamics, aerothermodynamics, propulsion, structures, weights, and other computations to produce point designs for a wide variety of launch vehicles. It is capable of iteratively sizing launch vehicles for specified missions. Although the trajectory guidance law is based on the energy-state model, the trajectory integration in HAVOC uses a point-mass model, including the effects of Earth rotation, Earth curvature, and variable gravity.

II. Methods

The three-dimensional aircraft point-mass equations of motion over a spherical, rotating Earth with no winds aloft, zero thrust, and terms in the square of the Earth rotation ignored are

$$\dot{X} = \frac{V R \cos\gamma \cos\chi}{(h+R)\cos(Y/R)}, \qquad \dot{Y} = \frac{V R \cos\gamma \sin\chi}{(h+R)}$$

$$\dot{h} = V\sin\gamma, \qquad \dot{V} = \frac{-D}{m} - g\sin\gamma$$

$$\dot{\gamma} = \left(\frac{L}{mV}\right)\cos\phi - \frac{g}{V}\cos\gamma + \frac{V}{(h+R)}\cos\gamma + 2\omega\cos\chi\cos\frac{Y}{R} \tag{1}$$

$$\dot{\chi} = \left(\frac{L}{mV\cos\gamma}\right)\sin\phi - \frac{V}{(h+R)}\cos\gamma\cos\chi\tan\frac{Y}{R} + 2\omega\left(\tan\gamma\sin\chi\cos\frac{Y}{R} - \sin\frac{Y}{R}\right)$$

For entry with zero thrust, the mass is constant. These equations, and the assumption $\dot{\gamma} = 0$, are used to obtain all of the numerical results in this paper.

Define the aircraft energy per unit weight by

$$E = [hR/(R+h)] + (1/2g_s)V^2 \tag{2}$$

Differentiate and use the state equations in Eqs. (1) to get

$$\dot{E} = -(VD/mg_s) = P \tag{3}$$

where P is the specific excess power.

Now replace V by E as state variable and use the observation that h and γ are capable of rapid change relative to E. The time rate of change of the flight-path angle $\dot{\gamma}$ and the altitude $\dot{h}$ are then neglected. This gives $\gamma = 0$, and the state equations become

$$\dot{X} = \frac{V R\cos\chi}{(h+R)\cos(Y/R)}, \qquad \dot{Y} = \frac{V R\sin\chi}{(h+R)}$$

$$\dot{E} = -\frac{VD}{mg} = P$$

$$0 = \frac{L}{mV}\cos\phi - \frac{g}{V} + \frac{V}{(h+R)} + 2\omega\cos\chi\cos\frac{Y}{R} \tag{4}$$

$$\dot{\chi} = \frac{L}{mV}\sin\phi - \frac{V}{(h+R)}\cos\chi\tan\frac{Y}{R} - 2\omega\sin\frac{Y}{R}$$

We will use this approximation, the ESA, throughout.

As mentioned earlier, this approximation has a long history of successful application in a wide variety of flight trajectory problems. The main drawback is that the variables h and γ may now jump instantaneously at points along the trajectory as well as at the boundaries. These jumps could be accounted for by boundary-layer analysis, but this is not done in this paper.

Minimum Time

To minimize the time to climb between two different pairs of altitude and velocity, with no boundary conditions specified on X, Y, or χ, it is clear that we must maximize $\dot{E}$ with respect to V for a given E subject to the fourth of Eqs. (4). The quantity to be minimized for a given energy gain is

$$J' = \int_{t_0}^{t_f} \mathrm{d}t = \int_{E_0}^{E_f} \frac{1}{P}\,\mathrm{d}E \tag{5}$$

where Eq. (3) was used and where the coupling with χ and Y caused by the Earth rotation (Coriolis) term in the fourth of Eqs. (4) is ignored. It is assumed that P is negative, E is monotonic, and the bank angle is zero.

For convenience, we choose to invert the integrand in Eq. (5) and to maximize; the quantity to be maximized is

$$J = \int_{E_0}^{E_f} P\,\mathrm{d}E \tag{6}$$

and thus the solution reduces to

$$\max_{h}\,(P)|_{E=\text{const}} \tag{7}$$

subject to the fourth of Eqs. (4) with $\omega = 0$ and $\phi = 0$ (no banking). This generates the well-known energy climb path.

Banking trajectories generally have higher lift and drag and thus may be expected to give shorter descent times. The optimization criterion in this case is

$$\max_{h,\,\phi}\,(P)|_{E=\text{const}} \tag{8}$$

A special case of banking is bank chattering (rapid switches in bank angle that leave $\cos\phi \neq 0$ and $\sin\phi = 0$). Now the criterion is

$$\max_{h,\,\phi}\,(P)|_{E=\text{const}} \quad \sin\phi = 0 \tag{9}$$

Minimum Heat Load

The quantity to be minimized for a given energy change in minimizing heat load is

$$J' = \int_{t_0}^{t_f} \dot{Q}\,\mathrm{d}t = \int_{E_0}^{E_f} \frac{\dot{Q}}{P}\,\mathrm{d}E \tag{10}$$

where Eq. (3) was used. $\dot{Q}$ is computed in HAVOC as a function of altitude, Mach number, and local angle of attack. It may be related to T_{surf} by considering a surface energy balance at a point on the

vehicle surface, which equates the convective heat rate with the radiative heat rate. This gives

$$\dot{Q} = e\sigma\left(T_{\text{surf}}^4 - T_{\text{amb}}^4\right) \tag{11}$$

If the weak dependence of e on T_{surf} is ignored, and noting that $T_{\text{surf}}^4 \gg T_{\text{amb}}^4$, this is approximately

$$\dot{Q} = e\sigma T_{\text{surf}}^4 \tag{12}$$

We choose to invert the integrand in Eq. (10) and to maximize; from Eqs. (10) and (12), the quantity to be maximized is

$$J' = \int_{E_0}^{E_f} \frac{P}{T_{\text{surf}}^4}\,\mathrm{d}E \tag{13}$$

and thus the solution reduces to

$$\max_{h}\left(\frac{P}{T_{\text{surf}}^4}\right)\bigg|_{E=\text{const}} \tag{14}$$

with $\phi = 0$ for no-banking trajectories. The optimization criterion in banking trajectories is therefore

$$\max_{h,\,\phi}\left(\frac{P}{T_{\text{surf}}^4}\right)\bigg|_{E=\text{const}} \tag{15}$$

and in the case of bank chattering the optimization problem is defined by

$$\max_{\substack{h,\,\phi \\ \sin\phi = 0}}\left(\frac{P}{T_{\text{surf}}^4}\right)\bigg|_{E=\text{const}} \tag{16}$$

As before, the fourth of Eqs. (4) is enforced.

Maximum Heading Change

To return to the launch site, in the event a mission must be aborted, the launch vehicle must be capable of executing turning trajectories with significant cross range. Inspection of Eqs. (4), however, shows that if cross range is to be maximized, then both E and χ must be retained as state variables and the single-state ESA approximation is not valid. Instead, to investigate turning capability we consider maximum heading angle change trajectories.

For maximum heading angle change trajectories, there is still coupling between the $\dot{E}$ and $\dot{\chi}$ state equations. The coupling occurs in the Earth curvature (centripetal) terms and in the Earth rotation (Coriolis) terms. Although the latter are relatively small effects, the centripetal terms are relatively large at the start of re-entry from orbit. The coupling in these terms must be ignored to obtain the ESA approximation. The quantity to be maximized is then

$$J' = \int_{\chi_0}^{\chi_f} \mathrm{d}\chi = \int_{t_0}^{t_f} \dot{\chi}\,\mathrm{d}t = \int_{E_0}^{E_f} \frac{\dot{\chi}}{P}\,\mathrm{d}E \tag{17}$$

where $\dot{\chi}$ is given by the last of Eqs. (4). In this case the optimization problem is therefore

$$\max_{h,\,\phi}\left(\frac{P}{-\dot{\chi}}\right)\bigg|_{E=\text{const}} \tag{18}$$

If the heading change reaches 90 deg relative to the deorbit value, a maximum range glide is initiated.

Maximum turning trajectories may result in excessive heating. For this reason, trajectories maximizing a weighted sum of negative heading change and heat load were also considered. In this case, the optimization problem is

$$\max_{h,\,\phi}\left(\frac{P}{K_1 T_{\text{surf}}^4 - K_2\dot{\chi}}\right)\bigg|_{E=\text{const}} \tag{19}$$

where K_1 and K_2 are mission-dependent weighting parameters to be determined empirically.

III. Numerical Results

All of the numerical examples are based on an SSTO rocket with a delta winged-body configuration.[2] The vehicle takes off vertically and lands horizontally. The minimum and maximum dynamic pressure limits were 20 and 900 psf, respectively. The temperature constraints at a point one-third of the way back from the nose are 1200°F for the upper surface and 1900°F for the lower surface. No stagnation heating constraints were imposed. The angle of attack was limited to 45 deg, and the maximum normal load factor was set to 2.5. Because of the high degree of nonlinearity of the vehicle model in HAVOC, all of the numerical searches [see, for example, Eq. (7)] are made by simply dividing the allowable altitude range into a large number of steps at each energy level and picking the one that results in the best value of the quantity being maximized. Additional numerical results may be found in Ref. 13. The first results to be presented are minimum time entry trajectories.

Minimum Time

Figures 1–4 illustrate the results from minimizing time. Four classes of trajectories were investigated: no banking, optimal left turn banking, optimal right turn banking, and optimal bank chattering [see Eqs. (7–9)].

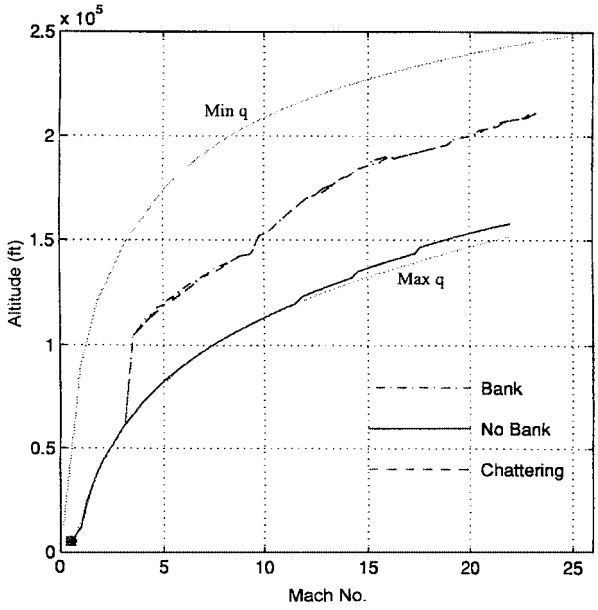

Fig. 1 Minimum time entry trajectories.

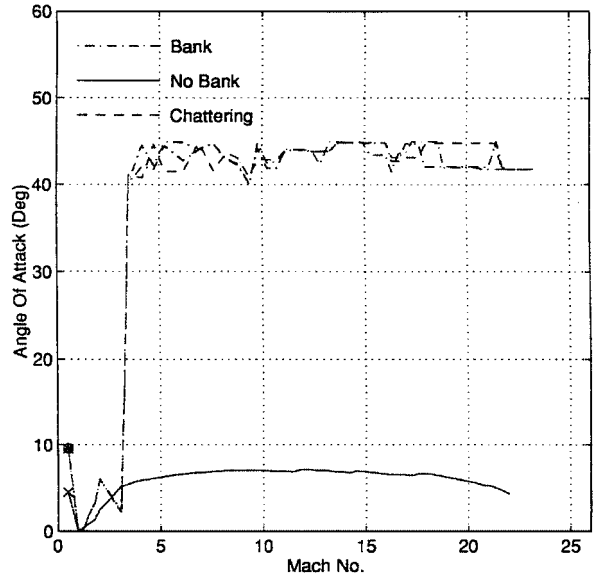

Fig. 2 Angle of attack for minimum time.

Table 1 Endpoint states of the optimized cases

Criteria	Time, s	Heat load, Btu/ft^2	Cross range, n mile
Positive banking (left turn)			
Min. time—no bank	661.00	6278.89	−65.20
Min. time—free bank	462.60	4653.32	268.20
Min. time—chattering	456.00	4573.55	−22.40
Min. temperature—no bank	2086.80	5491.00	−1837.60
Min. temperature—free bank	2013.80	5491.00	−1738.50
Min. temperature—chattering	2012.80	5491.00	−1820.40
Min. heat load—no bank	1478.20	4689.00	−788.30
Min. heat load—free bank	1327.20	4350.18	−145.90
Min. heat load—chattering	1345.90	4381.23	−441.50
Max. heading change—free bank	1255.20	8116.42	661.10
Negative banking (right turn)			
Min. time—no bank	661.00	6278.89	−65.20
Min. time—free bank	462.20	4639.91	−303.70
Min. time—chattering	456.00	4573.55	−22.40
Min. temperature—no bank	2086.80	5491.00	−1837.60
Min. temperature—free bank	2007.00	5450.63	−1824.20
Min. temperature—chattering	2012.80	5491.00	−1820.40
Min. heat load—no bank	1478.20	4689.00	−788.30
Min. haet load—free bank	1325.90	4340.88	−682.70
Min. heat load—chattering	1345.90	4381.23	−441.50
Max. heading change—free bank	1689.60	10059.66	−1254.80

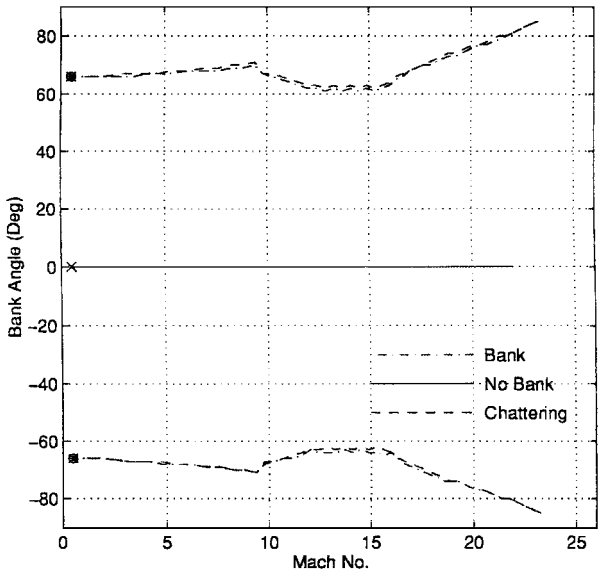

Fig. 3 Bank angle for minimum time.

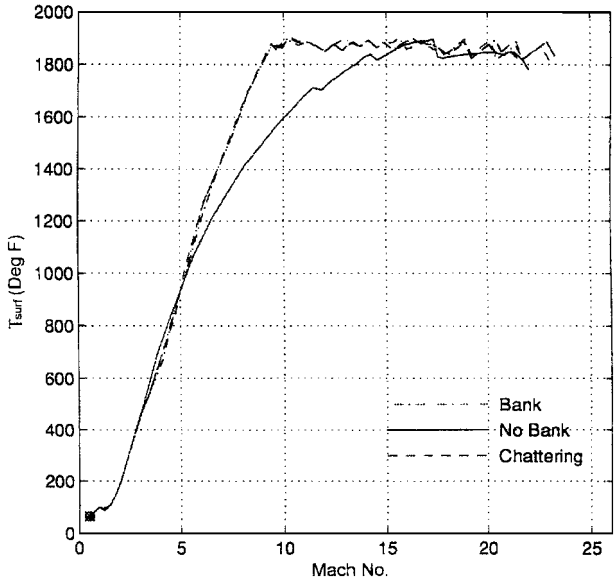

Fig. 4 Lower surface temperature (one-third back on windward side) for minimum time.

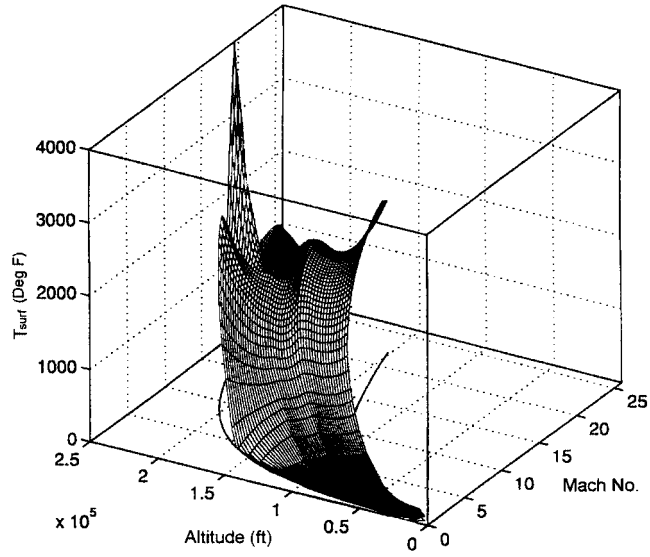

Fig. 5 Temperature contours (one-third back on windward side) of the minimum time no-banking case.

Figure 1 shows that the banking trajectories have much lower dynamic pressure than does the nonbanking one, and the latter one generally follows the maximum dynamic pressure q boundary. Table 1 shows that banking or bank chattering shortens the entry time by about 30% (200 s).

Figure 2 shows that the angle of attack of the banking trajectories is much higher than for the nonbanking ones, about 45 deg, the maximum value, as compared with 7 deg. The bank angle of the banking trajectories is in the range of 60–80 deg (Fig. 3) throughout the entire trajectory. If a stagnation heating constraint is imposed, the nonbanking trajectory would likely violate stagnation temperature limits.

Figure 4 shows the history of the lower surface temperature at the point on the windward side of the vehicle one-third of the way back from the nose. For all of the minimum time trajectories, this temperature is mostly at 1900°F, the upper imposed limit, for a significant portion of the trajectory.

Minimum Temperature

Vehicle temperature for vehicle normal equilibrium (one-third back on windward side) is plotted throughout the flight envelope on Figs. 5 and 6. Because of the complex aerothermal phenomena in the hypersonic regime, as modeled by HAVOC, these temperatures vary in a highly nonlinear way. In fact, there are two relative

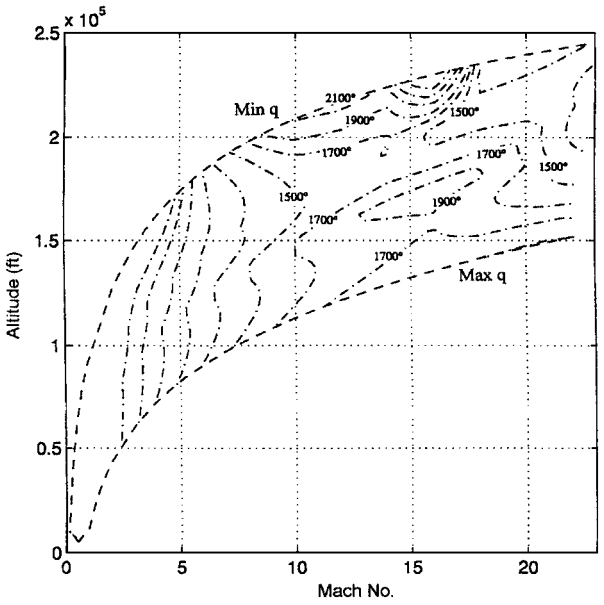

Fig. 6 Temperature mesh (one-third back on windward side) of the minimum time no-banking case.

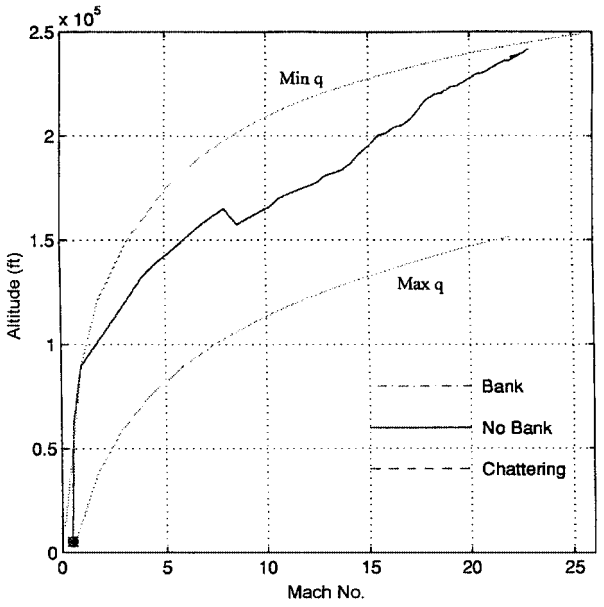

Fig. 7 Minimum temperature (one-third back on windward side) entry trajectories.

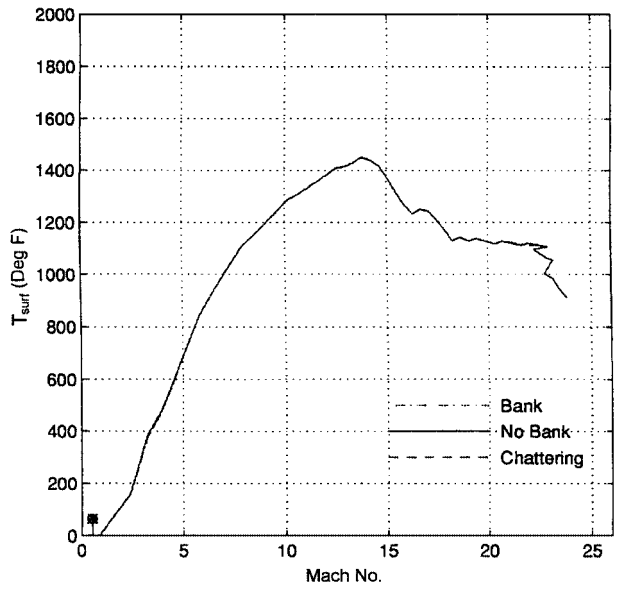

Fig. 8 Lower surface temperature (one-third back on windward side) for minimum temperature.

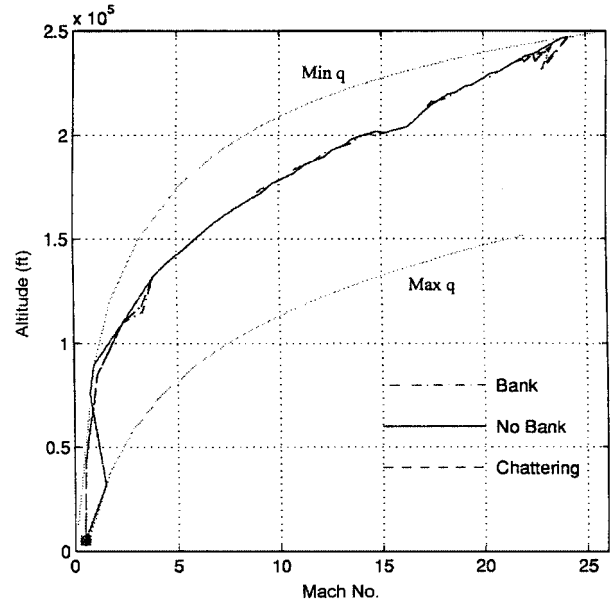

Fig. 9 Minimum heat load entry trajectories.

minimum temperature corridors, one at high q and low α, and one at relatively low q and high α, with the low q path giving slightly lower temperatures. Note that there are regions where the temperatures are higher than the maximum allowed 1900°F.

Figures 7 and 8 show minimum temperature trajectories. The path in the flight envelope (Fig. 7) follows the low q corridor of Figs. 5 and 6. Comparison of Figs. 4 and 8 shows that the maximum temperature relative to the minimum time trajectories has decreased substantially (to 1400°F). It was found that a significant portion of the minimum temperature path is near the maximum angle of attack of 45 deg and that, when the vehicle was allowed to bank, there was only a negligible amount of banking; thus nonbanking and banking trajectories are indistinguishable in Figs. 7 and 8. The minimum temperature trajectories are significantly longer in both downrange and time relative to the minimum time ones (5240 n miles downrange as compared with 1730 n miles and 2100 s as compared with 660 s; see Table 1).

Minimum Heat Load

One of the key objectives of an entry trajectory is minimizing heat load applied to the thermal protection system. In this paper the heat load has been approximated as the integral of vehicle surface temperature to the fourth power over time. Thus the minimum heating trajectories would be expected to be in some sense a compromise between the minimum time and the minimum temperature ones, tending more towards minimum temperature because of the fourth power in Eq. (13).

Comparison of Figs. 9 and 7 shows in fact that paths of the minimum heat load and minimum temperature trajectories are very similar. Figures 10 and 8 show that the temperatures are also very similar, but Table 1 shows that the times of the minimum heat load trajectories are significantly less, by about 600 s or 30%. In effect, the minimum heating trajectories attain very nearly minimum temperature but have considerably shorter times. This is accomplished by holding angle of attack at its maximum value for most of the flight and by employing a small amount of banking, never more than 20 deg. Table 1 shows that, relative to the minimum time banking and minimum temperature cases, the minimum heating cases have 6 and 20% less heat load, respectively.

Maximum Heading Change

Maximum heading angle change trajectories are shown in Figs. 11–15. A representative zero bank trajectory is shown for

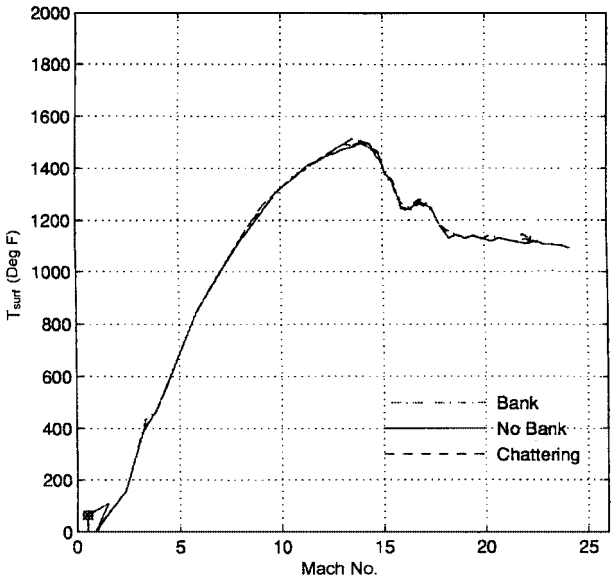

Fig. 10 Lower surface temperature (one-third back on windward side) for minimum heat load.

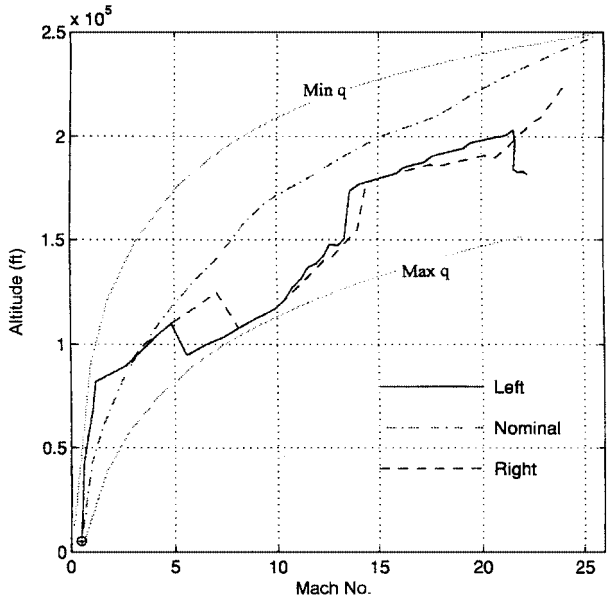

Fig. 11 Maximum heading angle change entry trajectories.

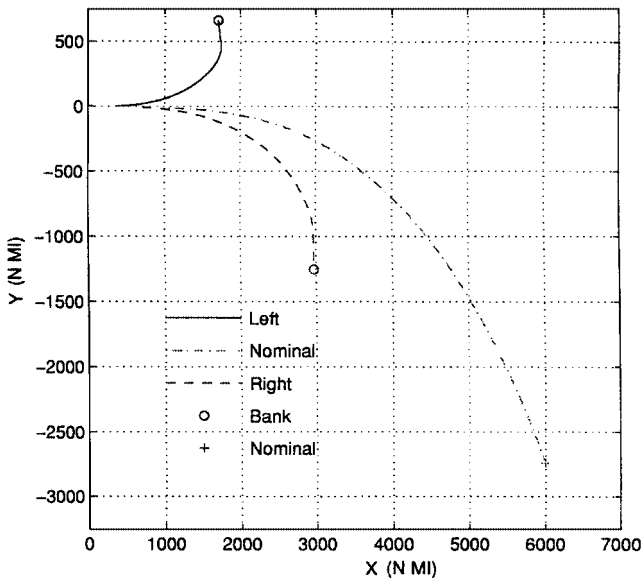

Fig. 12 Ground paths for maximum heading angle change.

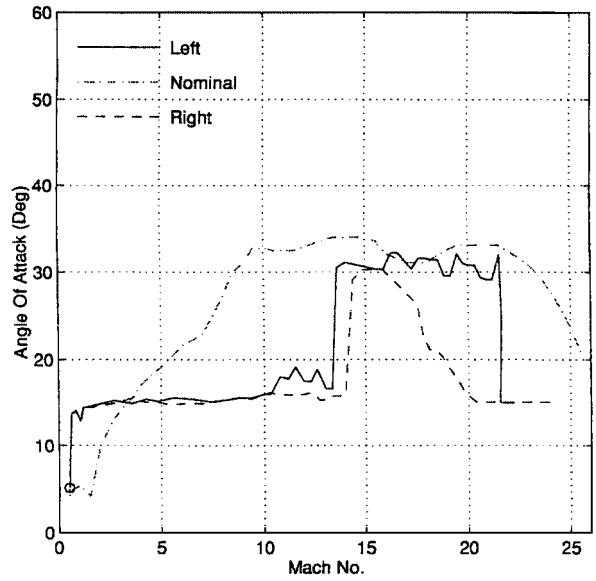

Fig. 13 Angle of attack for maximum heading angle change.

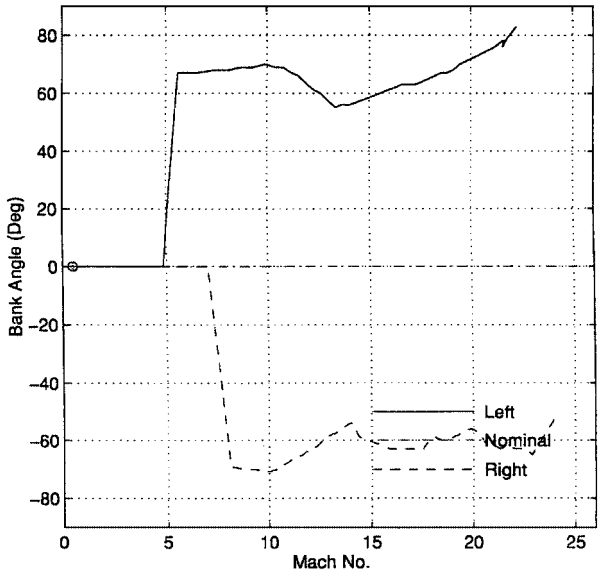

Fig. 14 Bank angle for maximum heading angle change.

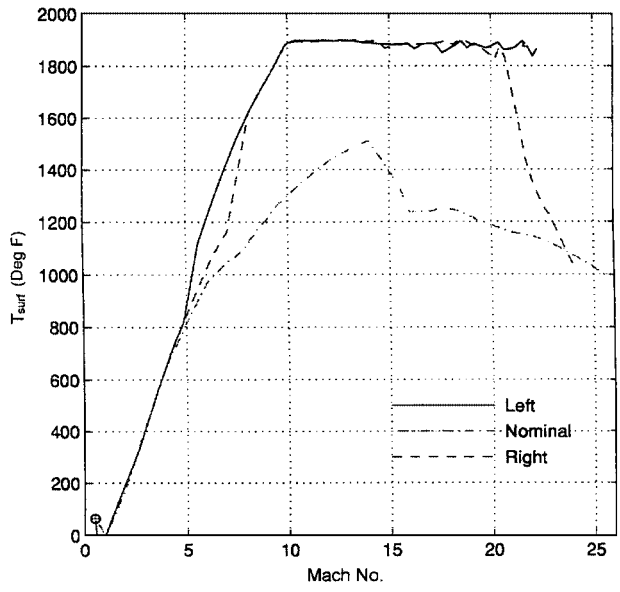

Fig. 15 Lower surface temperature (one-third back on windward side) for maximum heading angle change.

comparison (labeled Nominal). The interest in turning trajectories arises from abort requirements, particularly the need to return to the launch site after one orbit. Because turning increases vehicle surface temperatures, this abort trajectory is the case that typically sizes the thermal protection system. What is desirable is a flight path that results in sufficient cross range while minimizing heat load subject to temperature limits on the vehicle surface. As mentioned earlier, maximum cross-range problems do not reduce to energy-state approximation, and therefore maximum heading change trajectories are determined instead as an approximation. (When the heading change reaches 90 deg, the heading is held constant.) Although there is coupling between the $\dot{E}$ and $\dot{\chi}$ equations for maximum cross range, it is only through the centripetal and Coriolis terms, as mentioned earlier.

Figure 11 shows that the turning trajectories have higher q than the nominal and that they exhibit jumps in their paths. Figure 12 shows the ground paths of the three trajectories. Because of the use of curvilinear coordinates over the spherical Earth and the Earth's rotation, the zero bank trajectory has a curved ground path, and the right and left turns are not symmetrical.

Both the right- and left-hand turns are relatively hard, as shown by Figs. 13 and 14. The high-speed portion is flown at an angle of attack of about 30 deg, with a transition to about 15 deg at Mach number 13. For this vehicle, 15 deg is the angle of attack for maximum lift-to-drag (L/D) ratio, and thus the low-speed portion of the trajectories is at maximum L/D. This is in agreement with the classical result that maximum range in gliding flight is attained at maximum L/D. Both right and left turns have bank angles of 60–70 deg until supersonic speeds, when the bank angle is switched to zero for level gliding.

Figure 15 shows that the maximum heading angle change trajectories have maximum temperature for most of the flight. Table 1 shows that the turning trajectories take about the same time as the minimum heating trajectories but have from two to two-and-one-half times the heat load.

The parameter K_1 was held fixed and K_2 was varied [see Eq. (19)] to generate families of trajectories that are compromises between minimum heat load and maximum heading angle change. The results showed that about 400 n miles of cross range is possible with little or no increase in heat load. Beyond 400 n miles cross range, the heating rises steadily with cross range.

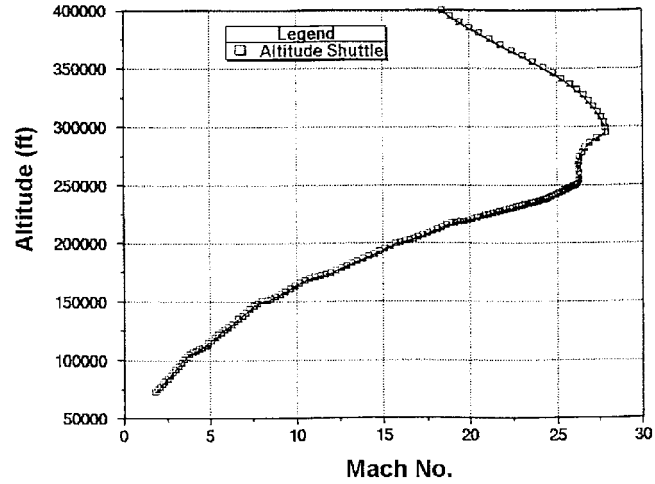

Fig. 16 Space Shuttle entry trajectories.

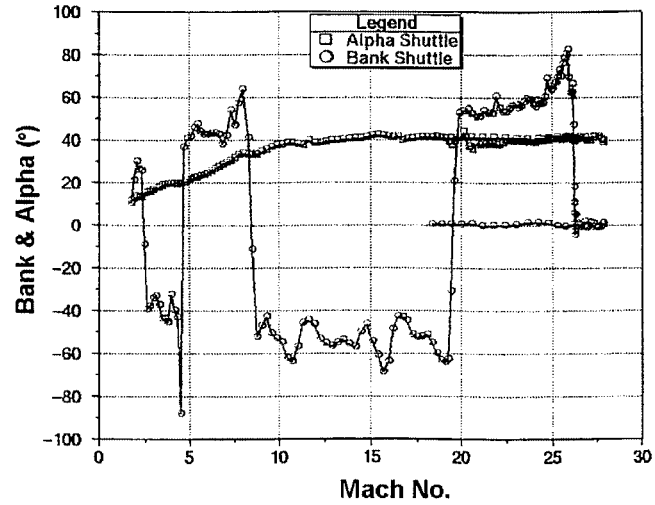

Fig. 17 Space Shuttle angle of attack and bank angle.

IV. Discussion

The purpose of the vehicle thermal protection system (TPS) is to limit internal structural temperatures in the vehicle to specified maximum values. This requires calculating the heat conducted to the interior surface of the TPS, which in turn requires a heat transfer analysis of the TPS. In our approach, this is approximated by considering the heat load at the outer, external surface. In Ref. 14, a finite difference solution of the one-dimensional heat equation is coupled to the ESA trajectory optimization routine and to HAVOC. The trajectories that minimize the interior temperature are shown to agree very closely with the trajectories determined in the present paper, indicating that maximizing the performance index in Eq. (13) gives a very good approximation.

In this paper, all of the numerical results were for a specific point on the vehicle surface, namely one-third back from the nose on the windward side of the vehicle. For a detailed vehicle design, these calculations would be done at grid points over the entire vehicle surface.

The dynamic model we have used, the energy-state approximation, allows instantaneous jumps in altitude at constant energy to occur. Inspection of Figs. 1, 7, 9, and 11 shows that some altitude jumps do occur, the largest one at supersonic speeds for the maximum heading angle change case (see Fig. 11). According to singular perturbation theory, these jumps occur on a faster timescale than the energy dynamics, and thus their impact on estimated performance may be expected to be slight. This is verified by Ref. 11, which investigates these jumps. For the more accurate calculations required for support of a detailed vehicle design, Eqs. (4) would need to be used with a numerical optimization code.

Finally, it is interesting to compare our results with Space Shuttle trajectories. Figures 16 and 17 show flight data from a Space Shuttle entry.[15] The entry trajectory (Fig. 16) begins with a segment of an elliptic transfer orbit, which ends when the sensible atmosphere is reached at an altitude of about 250,000 ft. Because this part of the trajectory is exoatmospheric, it does not contribute to the heating and therefore is of no interest here. Comparison of Fig. 16 with Figs. 1, 7, 9, and 11 shows that the trajectories obtained in the present paper are very similar to the atmospheric portion of the Space Shuttle trajectory.

The angle of attack and bank angle of the Space Shuttle's trajectory are shown on Fig. 17. The angle of attack is mostly at about 40 deg, in agreement with Fig. 2. The bank angle of the Space Shuttle osculates between about +60 and −60 deg, in agreement with Fig. 3 and approximating bank chattering.

V. Conclusions

The energy-state approximation was used to derive a near-optimal guidance law for entry trajectories of a SSTO rocket-powered launch vehicle. The guidance law was employed to obtain near-optimal entry trajectories for minimum time, minimum heat load, maximum heading angle change, and a combination of the latter two. Minimum temperature trajectories also were obtained.

A vehicle synthesis code using the guidance law was used to investigate SSTO entry performance. Numerical results show that nonbanking minimum time trajectories are quite different from minimum temperature trajectories. The former have much shorter times, much higher dynamic pressures, and much higher vehicle surface temperatures. When the vehicle was allowed to bank, the minimum time case banked at 60–70 deg, but the minimum temperature case did not bank.

Minimum heat load trajectories are intermediate between those of minimum time and minimum temperature, being more like the

latter. They achieve nearly minimum temperature but have significantly shorter times than the minimum temperature paths. Maximum heading change trajectories are partly at maximum lift-to-drag ratio and mostly at large values of bank angle. Finally, trajectories minimizing a weighted sum of heat load and cross range were considered. It was found that significant cross range is possible without significantly increasing heat load. The trajectories obtained agree generally with Space Shuttle flight data.

Acknowledgment

This work was supported by NASA Ames Research Center Grant NCC 2-5069.

References

[1]Bekey, I., "SSTO Rockets; A Practical Possibility," *Aerospace America*, Vol. 32, No. 7, 1994, pp. 32–37.

[2]Freeman, D. C., Talay, T. A., Stanley, D. O., Lepsch, R. A., and Wilhite, A. W., "Design Options for Advanced Manned Launch Systems," *Journal of Spacecraft and Rockets*, Vol. 32, No. 2, 1995, pp. 241–249.

[3]Roenneke, A. J., and Markl, A., "Re-Entry Control to a Drag-vs-Energy Profile," *Journal of Guidance, Control, and Dynamics*, Vol. 17, No. 5, 1994, pp. 916–920.

[4]Bradt, J., Langehough, M., and Robert, R., "Autonomous Guidance and Control for a Low L/D Crew Return Vehicle," AIAA Paper 91-2819, Aug. 1991.

[5]Kremer, J.-P., and Mease, K. D., "Near Optimal Control of Altitude and Path Angle During Aerospace Plane Ascent," *Journal of Guidance, Control, and Dynamics*, Vol. 20, No. 4, 1997, pp. 789–796.

[6]Corban, J. E., Calise, A. J., and Flandro, G. A., "Rapid Near-Optimal Aerospace Plane Trajectory Generation and Guidance," *Journal of Guidance, Control, and Dynamics*, Vol. 14, No. 6, 1991, pp. 1181–1190.

[7]Sachs, G., and Dinkelmann, M., "Heat Input Reduction in Hypersonic Flight by Optimal Trajectory Control," AIAA Paper 96-3905, July 1996.

[8]Ardema, M. D., Bowles, J. V., Terjesen, E. J., and Whittaker, T., "Near-Optimal Propulsion System Operation for Air-Breathing Launch Vehicles," *Journal of Spacecraft and Rockets*, Vol. 32, No. 6, 1995, pp. 951–956.

[9]Jansch, C., and Markl, A., "Trajectory Optimization and Guidance for a Hermes-Type Reentry Vehicle," AIAA Paper 91-2659, 1991.

[10]Ardema, M. D., Bowles, J. V., and Whittaker, T., "Optimal Trajectories for Hypersonic Launch Vehicles," *Dynamics and Control*, Vol. 4, No. 4, 1994, pp. 337–347.

[11]Ardema, M. D., Bowles, J. V., Terjesen, E. J., and Whittaker, T., "Approximate Altitude Transitions for High-Speed Aircraft," *Journal of Guidance, Control, and Dynamics*, Vol. 18, No. 3, 1995, pp. 561–566.

[12]Ardema, M. D., Chou, H.-C., and Bowles, J. V., "Near-Optimal Operation of Dual-Fuel Launch Vehicles," *Journal of Guidance, Control, and Dynamics*, Vol. 19, No. 5, 1996, pp. 1180–1182.

[13]Chou, H.-C., Ardema, M. D., and Bowles, J. V., "Near-Optimal Re-Entry Trajectories for Reusable Launch Vehicles," AIAA Paper 97-3582, Aug. 1997.

[14]Windhorst, R., Ardema, M. D., and Bowles, J. V., "Minimum Heating Re-Entry Trajectories for Advanced Hypersonic Launch Vehicles," AIAA Paper 97-3535, Aug. 1997.

[15]Hartung, L. C., and Thvockmorfor, D. A., "Space Shuttle Re-Entry Heating Data Book," NASA Reference Publication 1191, May 1988.